

Nondestructive characterization of $\text{Ga}_{1-x}\text{Al}_x\text{As-GaAs}$ interfaces using nuclear profiling

J. S. Rosner, P. M. S. Lesser, and F. H. Pollak

Physics Department, Brooklyn College of CUNY, Brooklyn, New York 11210

J. M. Woodall

IBM Thomas J. Watson Research Center, Yorktown Heights, New York 10598

(Received 16 April 1981; accepted 23 June 1981)

We present a new method for the nondestructive determination of the depth distribution of Al in $\text{Ga}_{1-x}\text{Al}_x\text{As-GaAs}$ heterostructures by means of nuclear profiling. This approach utilizes the $^{27}\text{Al}(p,\gamma)^{28}\text{Si}$ nuclear reaction which has an extremely sharp resonance width for protons incident at 992 keV. The presence of the Al is detected by means of the emitted 10.7 MeV γ ray. Depth profiling is accomplished by varying the energy of the incident proton beam. We have investigated the Al distribution of samples prepared using three different modifications of the liquid phase epitaxy method. Our results, after correction for straggling, are in good agreement with general considerations of the growth conditions.

PACS numbers: 73.40.Lq

I. INTRODUCTION

In compound semiconductor heterojunctions the variation of band gap near the surface and through the interface directly affect the optical and transport properties of the device. If an interface is abrupt, the band gap changes in a discontinuous manner, while if the interface is compositionally graded the band gap will change in a more gradual fashion. Recently, attempts to utilize the properties associated with band gap discontinuities at $\text{Ga}_{1-x}\text{Al}_x\text{As-GaAs}$ heterojunctions have required very stringent growth conditions during the formation of the interface.^{1,2} In addition, compositionally graded heterojunctions have been utilized for various purposes such as high efficiency $\text{Ga}_{1-x}\text{Al}_x\text{As-GaAs}$ graded band gap solar cells.³ Graded band gap layers can also be utilized to fabricate ohmic contacts.⁴ In order to understand the properties of such junctions it is necessary to have methods which characterize the interface region.

Depth profiling of Al in $\text{Ga}_{1-x}\text{Al}_x\text{As-GaAs}$ has in the past been performed by several methods including Auger electron spectroscopy, secondary ion mass spectroscopy, and Rutherford backscattering. The first two techniques are destructive since they involve removal of layers of the material by procedures such as ion milling.^{5,6} In addition, the ion milling itself may introduce experimental artifacts.^{5,6} Although Rutherford backscattering is nondestructive, it does not have very high resolution for the $\text{Ga}_{1-x}\text{Al}_x\text{As}$ system.³

In this paper we present a new method for the nondestructive determination of the Al distribution by means of nuclear profiling. This approach utilizes the $^{27}\text{Al}(p,\gamma)^{28}\text{Si}$ nuclear reaction which has an extremely sharp resonance (width ≈ 100 eV) for protons incident at 992 keV.⁷ The presence of the Al is detected by means of the emitted 10.7 MeV γ -rays. The depth profiling is accomplished by varying the energy of the incident proton beam. At an incident energy

of 992 keV only the Al nuclei near the surface are excited. At higher proton energies the beam must traverse a given amount of material until the energy is reduced to the value of 992 keV, which then enables it to interact with the Al. Thus, by varying the energy of the proton beam, the Al concentration is sampled at different depths in the heterojunction. We have investigated the Al distribution of samples grown by the three modifications of the LPE method which produce various profiles. Our results are in good agreement with general considerations of the growth conditions.^{8,9}

II. EXPERIMENTAL DETAILS

A. Sample growth conditions

The samples used in this study were p - p - n $\text{Ga}_{1-x}\text{Al}_x\text{As-GaAs-GaAs}$ solar cell structures. The structures were prepared using three different modifications of the liquid phase epitaxy (LPE) method. These conditions are illustrated by the phase diagram in Fig. 1(a). To form the structures, $\text{GaAs}(100)$ oriented substrates with $n = 1-2 \times 10^{17} \text{ cm}^{-3}$ are placed in contact with melts of Ga-Al-As doped with Mg to produce a p -type carrier concentration in the GaAs layer of about $1 \times 10^{18} \text{ cm}^{-3}$. The melts have one of the phase conditions A , B , or C . Shown in the lower portion of the figure is a schematic representation of the various regions of the p - p - n $\text{Ga}_{1-x}\text{Al}_x\text{As-GaAs-GaAs}$ structures.^{8,9} The strains at the $\text{Ga}_{1-x}\text{Al}_x\text{As-GaAs}$ interface of similar configurations have recently been investigated using electrolyte electroreflectance (EER).¹⁰ A value of $x \approx 0.9$ can be deduced from the growth conditions and has been verified by EER measurements of various optical transitions.^{10,11} In all three instances the combined thickness of the transition region plus the $\text{Ga}_{1-x}\text{Al}_x\text{As}$ layer is expected to be $\approx 0.5 \mu\text{m}$.

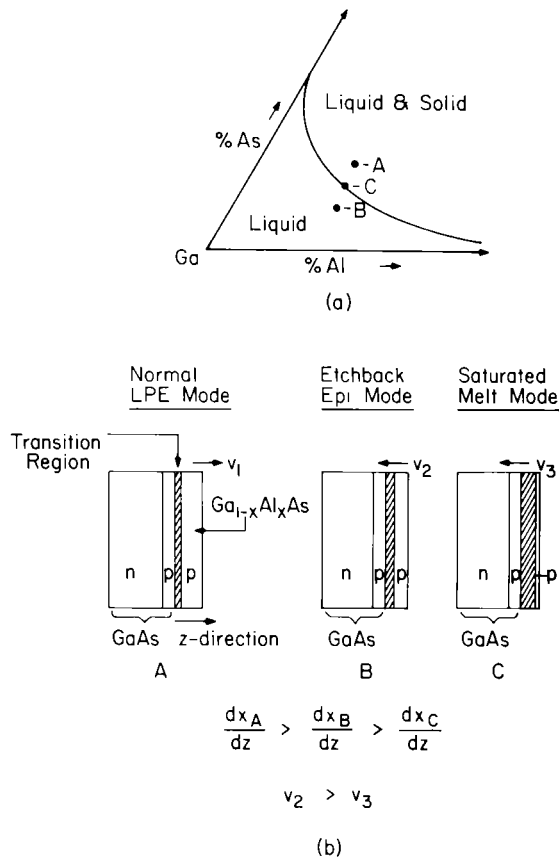


FIG. 1. (a) Schematic representation of the phase diagram for the liquid phase epitaxy growth conditions used for the $Ga_{1-x}Al_xAs$ layers. (b) Schematic drawings of the various regions of the $p-p-n Ga_{1-x}Al_xAs-GaAs-GaAs$ heterostructures. Indicated are relative magnitudes of the concentration gradient dx/dz for the three cases.

Melts of type A (normal LPE mode) are initially in a solid-liquid two phase region and hence all are supersaturated. When the GaAs substrate contacts type A melts there is a strong driving force for solid phase precipitation, i.e., growth of a p -type layer of $Ga_{1-x}Al_xAs$, at a velocity v_1 . This gives rise to a relatively thin transition region [see Fig. 1(b)] in which the composition changes from GaAs to $Ga_{1-x}Al_xAs$ and, hence, produces a relatively high concentration gradient and large strain at the interface. As the p -type $Ga_{1-x}Al_xAs$ layer grows, Mg diffuses into GaAs substrate forming a p -region.

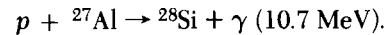
Melts of type B (etchback epi mode) are initially undersaturated. When a GaAs substrate contacts this type of melt, the GaAs begins to dissolve into the melt in an attempt to bring the melt to two phase equilibrium. The continuous movement of solid-liquid interface towards the solid direction at a velocity v_2 creates a situation of diffusion occurring under a moving boundary condition. This growth condition has been treated theoretically for the case of Ga-Al-As melts.⁹ The result is that Al diffuses into GaAs along with the Mg dopant and produces a transition region which is thicker than that for type A melts and hence produces a smaller concentration gradient.

Melts for type C (saturated melt mode) are initially at two phase equilibrium. When a GaAs substrate is placed in contact with this melt, dissolution at rate v_3 is also expected to occur but at a lower rate. This results in the widest transition region

of the three conditions. The relative magnitudes of the concentration gradient, dx/dz , for the three growth cases are indicated in Fig. 1(b).

B. Nuclear profiling technique

The Al profiling technique makes use of the nuclear reaction:



There is a very narrow isolated resonance in the cross section for this reaction at a proton energy E_p of 992 ± 0.10 keV (laboratory). Hence, if a sample is bombarded with protons at the resonance energy, the yield of 10.7 MeV characteristic γ -rays is proportional to the amount of Al at the surface of the material. If the beam energy is raised, the yield of γ -rays from the reaction with Al near the surface will be negligible because the protons are above the resonance energy as they penetrate the solid and reach the resonance energy at some depth. Now the yield of characteristic γ -rays is proportioned to the Al at this depth. Hence, by measuring the γ -ray yield vs proton beam energy the distribution of Al as a function of depth z is determined.

The material to be investigated was bombarded with protons in an appropriate energy range generated by the Brooklyn College Dynamitron Accelerator. The sample was mounted at the end of the beam pipe which had a vacuum of $\approx 10^{-6}$ Torr (1.33×10^{-4} Pa). The beam current used was approximately 0.5 microamperes and had a spot size of about 10 mm² in cross section. This value of the beam flux was chosen to be low enough so as to avoid heating but yet was sufficient to produce a statistically significant number of γ -rays. In addition, this value of the flux introduced less than 10^{13} cm⁻³ transmuted ²⁸Si nuclei during the operating time and hence is well into the nondestructive regime. The emitted 10.7 MeV γ -rays were counted by means of a NaI detector with dimensions 3 inches thick and 3 inches in diameter. The detector was placed about 1 cm from the target material and oriented at zero degrees; i.e., γ -rays in the forward direction were counted.

In order to calculate the beam energy loss in traversing a given thickness of sample, the following relation is used:

$$E_0 = E_r + \int_0^z \left(\frac{dE}{dz'} \right) dz' \quad (1)$$

where E_0 and E_r are the beam energy and resonance energy (992 keV), respectively, and dE/dz is the rate of energy loss of protons in the solid. For the samples used in this investigation it was found that the proton beam lost no more than about 50 keV in going through the $Ga_{1-x}Al_xAs$ section. Therefore, it was sufficient to use a linear fit to dE/dz ; i.e.,

$$dE/dz = a - bE, \quad (2)$$

where the parameters a and b were determined from the tabulated data in Northcliffe and Schilling¹² for protons in Al and Ge. The stopping power of Ge was used in place of Ga and As³ and Bragg's rule¹³ was employed to calculate the stopping power in the composite material, $Ga_{1-x}Al_xAs$, for a given concentration of Al. Then, by numerical integration, the depth $z(E_0)$ could be calculated for which the energy loss

equaled the difference between the incident beam energy, E_0 , and the resonant energy, E_r . In this manner, the measured gamma ray yield $Y_\gamma(E_0)$, could be translated into a corresponding depth profile of Al, $\rho_{Al}(z)$, in the sample. This entire procedure can be iterated so as to allow for the varying concentration of Al in the sample insofar as it affects the calculated energy loss, i.e., the relationship between z and E_0 . In practice, a single iteration was sufficient. Although the measured gamma ray yield can in principle provide an absolute measure of the Al concentration, we have used the technique to obtain an accurate determination of only the relative Al concentration as a function of depth. The absolute value of $x \approx 0.9$ at the maximum region was obtained from the EER measurement^{10,11} and is consistent with the growth conditions.

The Al profile obtained in the manner outlined above does not yet represent the true distribution in the sample due to several effects which tend to broaden the measured profile. Principal among these is the effect of energy straggling which results from the statistical nature of the energy loss mechanism as the beam traverses a given thickness of material.¹⁴ Thus, the beam energy at depth z in the sample is not sharply defined but rather has an approximately Gaussian distribution whose width Δ_s is a function of z . This width can be calculated using the Bohr formula.¹⁴

$$\Delta_s = 2.35 (4\pi e^4 Z_1^2 Z_2 N z)^{1/2} \quad (3)$$

where Z_1 and Z_2 represent the projectile and target atomic numbers respectively, N is the atomic density of the stopping medium, and z is the thickness.

For a composite stopping material, a formula suggested by Chu and analogous to the Bragg rule can be used.¹⁴ According to Chu, the Bohr formula tends to overestimate the energy straggling width for $Z_2 \gtrsim 10$ and $E_p \approx 1$ MeV, although the experimental data are not sufficiently good to verify this theory. In the present case, however, Chu's theory gives a result for the straggling width which is only $\approx 10\%$ less than the Bohr formula, so the uncertainty in this result is small. For example, we calculate for $E_p = 1$ MeV in $Ga_{1-x}Al_xAs$ (average $Z_2 \approx 24$), a straggling width Δ_s equal to (5.0 ± 0.5) keV at a depth of 2000 Å in the sample, etc. At the surface of the sample, of course, the straggling width is negligibly small.

In addition to broadening due to energy straggling, there is a constant instrumental width (Δ_0) of ≈ 1 keV (FWHM) due to the energy spread of the incident proton beam. This effect broadens the measured profile at the surface of the sample as well as at any depth in the sample.

Broadening, due to the inherent width of the resonance, is completely negligible in this case since the resonance width (FWHM) is only 100 eV for $^{27}Al(p,\gamma)^{28}Si$ at $E_p = 992$ keV. Contributions to the gamma ray yield from the next (lower energy) resonance were present only in the case of the thickest sample measured and this contribution was subtracted out on the basis of the measured thin sample yield function.

An exact determination of the true aluminum profile requires a deconvolution of the integral,

$$Y_\gamma(E_0) = A \int_0^\infty dz' \rho_{Al}(z') \times \exp\{-[E_r - \bar{E}(z')]^2 / [\Delta_0^2 + \Delta_s^2(z')]\}, \quad (4)$$

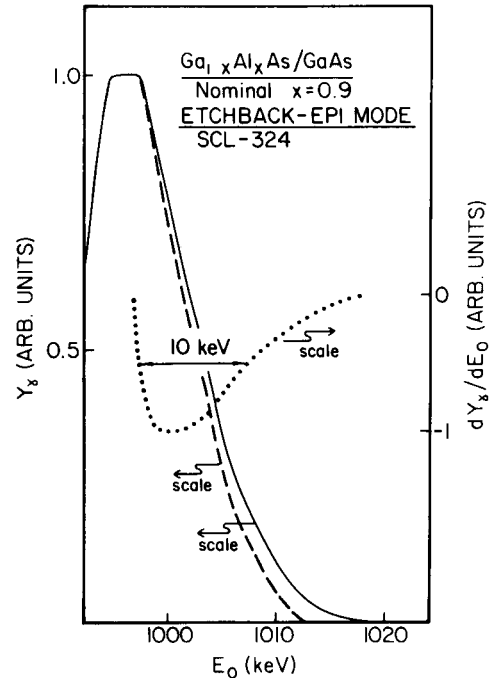


FIG. 2. Experimentally measured gamma-ray yield, Y_γ (solid line), and its derivative, dY_γ/dE_0 (dotted line), as a function of incident proton energy, E_0 , for sample SCL-324. The dashed line represents the yield after correction for straggling and instrumental effects.

where $Y_\gamma(E_0)$ is the measured gamma-ray yield as a function of incident proton energy (E_0), $\rho_{Al}(z)$ is the depth distribution of Al in the sample, $E(z)$ is the mean beam energy at depth z in the sample, Δ_0 is the instrumental width, and $\Delta_s(z)$ is the straggling width [see Eq. (3)]. The above expression assumes the existence of a single very narrow resonance in the $^{27}Al(p,\gamma)^{28}Si$ reaction.

To analyze the present data we have adopted a simplified procedure suitable for extracting the gross features of the aluminum profile, rather than attempting a complete deconvolution. In this procedure, we plot the derivative of the measured yield, dY_γ/dE_0 , and extract from this plot the widths of the yield function at the interface between the $Ga_{1-x}Al_xAs$ and $GaAs$. This measured width, Δ_m , can be presumed to be composed of several components (Al distribution, instrumental, straggling) adding in quadrature. Thus

$$\Delta_m^2 = \Delta_{Al}^2 + \Delta_s^2 + \Delta_0^2, \quad (5)$$

where Δ_{Al} is the Al distribution. By subtracting the known instrumental width and the straggling width (calculated as outlined above) from the measured width, we can then determine (to a reasonable degree) the true profile of the Al distribution.

Shown in Fig. 2 is the measured gamma ray yield Y_γ (solid line) and its derivative dY_γ/dE_0 (dotted line), as a function of incident proton energy E_0 for sample SCL-324. This material was grown under condition B in Fig. 1. The parameter Δ_m can be evaluated from the FWHM of dY_γ/dE_0 in the interfacial region. For this sample $\Delta_m = 10$ keV. The minimum in the dY_γ/dE_0 curve occurs at $E_0 \approx 1000$ keV (see Fig. 1), which from Eqs. (1) and (2) corresponds to a depth of about 2000 Å. Hence, from Eq. (3) the straggling parameter $\Delta_s = 5$ keV at this depth. As mentioned before $\Delta_0 = 1$ keV. Thus,

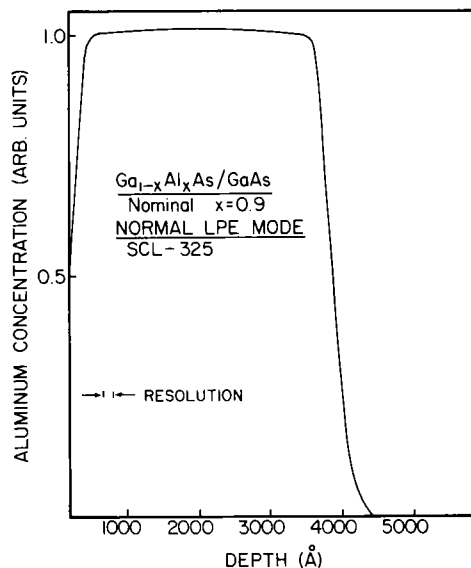


FIG. 3. Aluminum concentration (in arbitrary units) as a function of depth for sample SCL-325 which was fabricated in the normal LPE mode. The maximum height of the curve corresponds to the nominal composition $x \approx 0.9$. The resolution is related to the energy spread of the incident beam.

we deduce from Eq. (5) that the above values of Δ_s and Δ_0 represent a 15% correction to the measured yield. This is indicated by the dashed line in Fig. 2, which now gives a reasonably valid profile of the Al distribution in this sample.

III. EXPERIMENTAL RESULTS

Plotted in Fig. 3 is the Al depth profile of sample SCL-325 which was grown in the "normal LPE" mode, i.e., condition A as indicated in Fig. 1. The resolution limit of about 130 Å corresponds to the instrumental width (Δ_0) of 1 keV. Except for the section near the surface (we shall return to this point later) the Al concentration ($x \approx 0.9$) is quite uniform over a width of about 3000 Å. The transition region, which begins

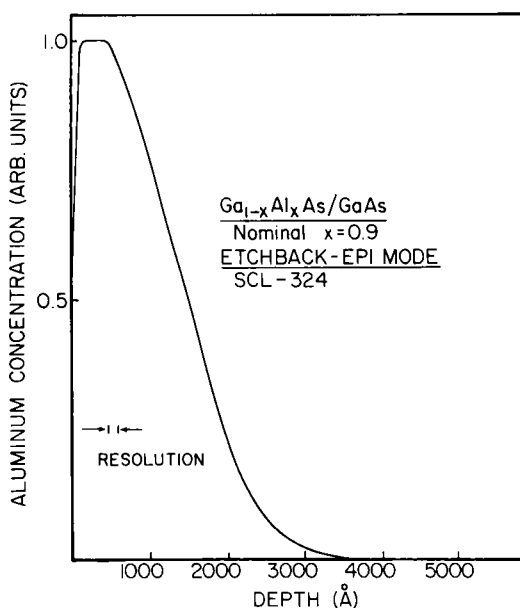


FIG. 4. Aluminum concentration (in arbitrary units) as a function of depth for sample SCL-324 which was fabricated in the etchback-epi mode. The maximum height of the curve corresponds to the nominal composition $x \approx 0.9$. The resolution is related to the energy spread of the incident beam.

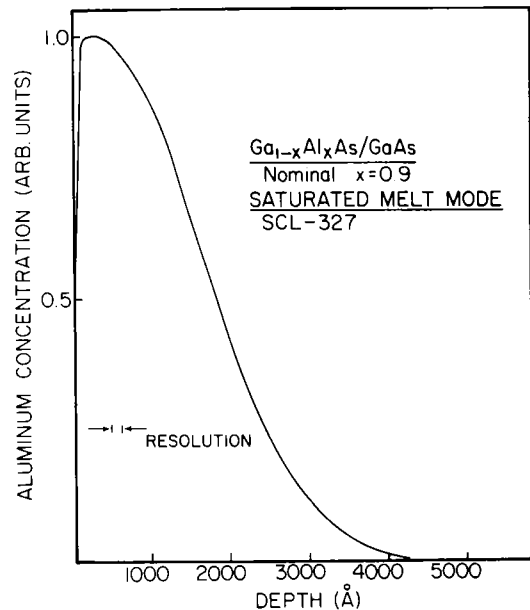


FIG. 5. Aluminum concentration (in arbitrary units) as a function of depth for sample SCL-327 which was fabricated in the saturated melt mode. The maximum height of the curve corresponds to the nominal composition $x \approx 0.9$. The resolution is related to the energy spread of the incident beam.

at a depth of about 3500 Å, is fairly abrupt, being about 500 Å wide.

Displayed in Fig. 4 are the results for sample SCL-324, which was fabricated using the "etchback-epi" mode (condition B in Fig. 1). For this material the $\text{Ga}_{0.1}\text{Al}_{0.9}\text{As}$ plateau section is only about 500 Å in width while the transition region occurs over about 2500 Å. Thus this junction is more gradual than that of sample SCL-325.

The depth profile for sample SCL-327 is shown in Fig. 5. This material was grown using the "saturated melt" mode, which is designated condition C in Fig. 1. Note that there is almost no plateau where $x \approx 0.9$ and that the transition region is about 3500 Å wide.

In all three samples there appears to be a decline in the Al concentration from $x \approx 0.9$ in a narrow region near the surface. At present we do not know whether or not this effect is real. Note that this narrow region corresponds approximately to the resolution width and hence may simply represent the corresponding uncertainty in determining where the "surface" is. There may be a thin oxide layer on the surface. This could produce an apparent change in Al concentration since the oxide would have a different Al content and density in relation to the $\text{Ga}_{1-x}\text{Al}_x\text{As}$. Or the effect may indeed be real. The above considerations are under further investigation.

IV. CONCLUSIONS

The results of this study clearly demonstrate the usefulness of nuclear profiling in nondestructively determining the Al profile in $\text{Ga}_{1-x}\text{Al}_x\text{As}$ -GaAs heterojunction structures. It shows the strong dependence of the Al distribution on small changes in the LPE growth mode. These factors are obviously of considerable importance for the fabrication of various heterostructure devices such as abrupt¹ or graded band gap³ solar cells, injection lasers,² etc. It is thus possible to tailor the nature

of the interface and "plateau" regions by the appropriate choice of growth conditions.

The various experimentally determined Al depth profiles are in good agreement with the models of the growth circumstances,^{8,9} e.g., condition A yields the largest dx/dz while the C mode produces the smallest dx/dz . The profiling results also show a good correlation with the experimentally determined strains at the $\text{Ga}_{1-x}\text{Al}_x\text{As-GaAs}$ interface. The most gradual heterojunction interface (saturated melt mode) shows no interfacial strain while both the etchback epi and normal LPE modes reveal strains which are approximately equal to the lattice mismatch.¹⁰

It should be pointed out that the nuclear profiling technique is well suited for topographical studies. The proton beam can easily be focused to a spot size of at least $100\ \mu\text{m}$. It would then be possible to determine if the depth distribution of the Al were uniform corresponding to different points on the surface of the sample.

ACKNOWLEDGMENTS

We wish to thank W. K. Chu for some extremely valuable discussions concerning corrections for straggling. Fred H.

Pollak acknowledges the support of the Office of Naval Research under contract NOOO 14-78-C-0890.

¹See, for example, H. Hovel, *Solar Cells, Semiconductors and Semimetals*, Vol. 11 (Academic, New York, 1975).

²See, for example, A. G. Milnes, and D. L. Feucht, *Heterojunctions and Metal-Semiconductor Junctions* (Academic, New York, 1972).

³See, for example, R. Sahia, J. S. Harris, D. D. Edwall, and F. H. Eisen, *J. Electron. Mater.* **6**, 645 (1977) and references therein.

⁴J. M. Woodall, J. L. Freeouf, G. D. Pettit, T. Jackson, and P. Kirchner, these proceedings.

⁵See, for example, C. M. Garner, C. Y. Su, and W. E. Spicer, *J. Vac. Sci. Technol.* **16**, 1521 (1979); P. S. Ho, *Surf. Sci.* **85**, 19 (1979).

⁶See, for example, W. K. Chu, M. A. Nicolet, J. W. Mayer, and C. A. Evans, *J. Anal. Chem.* **46**, 2136 (1974).

⁷See, for example, E. Wolicki in *New Uses of Ion Accelerators* (Plenum, New York, 1975), p. 159.

⁸P. Kordos, G. L. Pearson, and M. B. Panish, *J. Appl. Phys.* **50**, 6902 (1979).

⁹M. B. Small and R. Ghez, *J. Appl. Phys.* **50**, 5322 (1974).

¹⁰F. H. Pollak and J. M. Woodall, *J. Vac. Sci. Technol.* **17**, 1108 (1980).

¹¹O. Berolo and J. C. Woolley, *Can. J. Phys.* **49**, 1335 (1971).

¹²L. C. Northcliffe and R. F. Schilling, *Nuclear Data Tables A7*, 233 (1970).

¹³See, for example, W. K. Chu in *Ion Beam Handbook for Materials Analysis* (Academic, New York, 1977), p. 2.

¹⁴W. K. Chu, *Phys. Rev. A* **13**, 2057 (1976).